Holes in the t-J_z model: A diagrammatic study

A. L. Chernyshev*
Physics Department, University of California, Riverside, California 92521

P. W. Leung
Physics Department, Hong Kong University of Science and Technology, Clear Water Bay, Hong Kong, China
(Received 25 January 1999)

The t-J_z model is the strongly anisotropic limit of the t-J model which captures some general properties of doped antiferromagnets (AF's). The absence of spin fluctuations simplifies the analytical treatment of hole motion in an AF background, and allows us to calculate single- and two-hole spectra with a high accuracy using a regular diagram technique combined with a real-space approach. At the same time, numerical studies of this model via exact diagonalization on small clusters show negligible finite-size effects for a number of quantities, thus allowing a direct comparison between analytical and numerical results. Both approaches demonstrate that the holes have a tendency to pair in p- and d-wave channels at realistic values of t/J. Interactions leading to pairing and effects selecting p and d waves are thoroughly investigated. The role of transverse spin fluctuations is considered using perturbation theory. Based on the results of the present study, we discuss the pairing problem in the realistic t-J-like model. Possible implications for preformed pairs formation and phase separation are drawn. [S0163-1829(99)04127-2]

I. INTRODUCTION

The physics of holes moving in an antiferromagnetic (AF) background has received much attention because of its possible connection to high-T_c superconductivity. A microscopic realization of this physics is given by the t-J model, which was first introduced as a conjecture,[1] and then derived as a low-energy limit of a realistic model representing the electronic structure of cuprates.[2,3] Recent comparison of the t-J model results to angle-resolved photoemission data[4] showed that the overall shape of the experimental single-hole band can be fitted satisfactorily using the pure t-J model. To account for the detail line shapes, one needs to include more distant hopping terms (t', t'', etc.).[5,6] The presence of these terms also follows from a careful mapping study.[6] Numerical studies of the t-J model by means of exact diagonalization (ED) and other methods suggest the presence of hole binding in the physical parameter range $t/J \sim 3$,[7–9] and that the dominant symmetry of the pairing correlation is $d_{x^2-y^2}$. This finding also supports the common belief that some variant of the t-J model is able to describe the physics of real compounds. However, to show that this d-wave binding in the t-J model is relevant to the physics of high-T_c materials, one has to clarify how strong and generic the reasons behind this pairing are. Unfortunately, numerical studies alone are of limited use for this purpose, so that an analytical study is necessary to develop insight into the problem.

In this paper we attempt such a study by investigating the Ising limit of the t-J model — the t-J_z model. This is well known to be a simplified limiting case of the t-J model, but only recently has its properties been fairly well understood. In the pioneering work of Ref. 10, the single-hole energy in the $t/J \ll 1$ limit has been calculated. Subsequently, Brinkmann and Rice[11] considered the $J=0$ limit, and introduced the retraceable-path approximation. In infinite dimensions [$d=\infty$] both the retraceable-path approximation and the t-J_z model become an exact description of the t-J model,[12] which supports the idea that the results of the strongly anisotropic limit of the t-J model are relevant to the physics of the isotropic case in $d=2$. More recent works[13–17] used the self-consistent Born approximation to study the t-J_z, t-J, and t-t'-J models. Using this approximation, an analytical expression for the hole Green's function in the t-J_z model for arbitrary values of t/J was found by Starykh and Reiter.[18] The pairing of holes in the t-J_z model was considered in the works by Trugman[19] and Shraiman and Siggia,[20] where important results were obtained. Some other studies used different modifications of the variational approach,[21,22] and obtained similar results. However, as we shall show, these earlier analytical treatments involved approximation which prevented one from obtaining the correct answers.

The t-J_z model was studied using numerical methods.[7] Barnes *et al.*[23] compared their ED results on a 16-site square lattice with some analytical results, and Riera and Dagotto[24] developed a modified Lanczos technique which enabled them to study the one- and two-hole ground states of the model on lattices as large as 50 sites. (For a review, see Ref. 7). It was shown that finite-size effects in the ED data of the t-J_z model are much smaller than those of the t-J model.[24]

In this paper we develop an analytical treatment of the t-J_z model based on the results of Ref. 18. Comparison with our ED data allows us to justify the validity of this analytical approach. Furthermore, we use the results of this study to shed light on the problem of whether the pairing in the d channel is a generic feature of t-J-like models, and which interaction defines the symmetry of the ground state of the system. Qualitatively similar questions have been addressed in a recent variational study of the hole pairing in the t-J model.[25]

Our numerical ED results for the t-J_z model are obtained

on a 32-site square lattice using the same method as in Refs. 26 and 27. Up to now these are the only ED results on the largest lattice. This numerically exact method allows us to analyze various properties of the single-hole ground state as well as two-hole bound states with different symmetries.

Our paper is organized as follows. Sections II and III describe the representation and Feynman rules used in this paper. In Sec. IV we solve the single-hole problem and compare the results to ED data. In Sec. V the two-hole problem is considered in detail. In Sec. VI we summarize our results and draw conclusions.

II. Hamiltonian and Representation of the Operators

The Hamiltonian of the t-J_z model is

$$\mathcal{H}=-t\sum_{\langle ij\rangle\sigma}(\tilde{c}^{\dagger}_{i\sigma}\tilde{c}_{j\sigma}+\text{H.c.})+J\sum_{\langle i,j\rangle}[S^z_iS^z_j-\tfrac{1}{4}N_iN_j], \quad (1)$$

where the summation runs over nearest-neighbor bonds $\langle ij\rangle$, $\tilde{c}^{\dagger}_{i\sigma}=c^{\dagger}_{i\sigma}(1-n_{i\bar{\sigma}})$, $\tilde{c}_{i\sigma}=(\tilde{c}^{\dagger}_{i\sigma})^{\dagger}$, and $N_i=\tilde{c}^{\dagger}_{i\uparrow}\tilde{c}_{i\uparrow}+\tilde{c}^{\dagger}_{i\downarrow}\tilde{c}_{i\downarrow}$. Since we are modeling electrons on a two-dimensional square lattice, the coordination number $z=4$ and the spin $S=\frac{1}{2}$.

Assuming the presence of long-range antiferromagnetic order, one can introduce a representation for the Hubbard operators (operators of spin and constrained fermion) through the spinless fermion and boson operators. The choice of the representation is, in general, arbitrary, and is motivated by the problem to be solved. In our work we use a generalization of the Dyson-Maleev (DM) representation for the Hubbard operators. As usual, such a representation conserves the algebra of the operators but extends the Hilbert space of the problem.

In sublattice $A=\{\uparrow\}$ the DM representation is given by

$$\begin{aligned}
&S^z_i=\tfrac{1}{2}(X^{\uparrow\uparrow}_i-X^{\downarrow\downarrow}_i)=\tfrac{1}{2}-a^{\dagger}_ia_i-\tfrac{1}{2}f^{\dagger}_if_i,\\
&S^-_i=X^{\downarrow\uparrow}_i=a^{\dagger}_i(1-a^{\dagger}_ia_i-f^{\dagger}_if_i),\quad S^+_i=X^{\uparrow\downarrow}_i=a_i,\\
&\tilde{c}_{i\uparrow}=X^{0\uparrow}_i=f^{\dagger}_i(1-a^{\dagger}_ia_i),\quad \tilde{c}^{\dagger}_{i\uparrow}=X^{\uparrow 0}_i=f_i,\\
&\tilde{c}_{i\downarrow}=X^{0\downarrow}_i=f^{\dagger}_ia_i,\quad \tilde{c}^{\dagger}_{i\downarrow}=X^{\downarrow 0}_i=f_ia^{\dagger}_i,\\
&N_i=\tilde{c}^{\dagger}_{i\uparrow}\tilde{c}_{i\uparrow}+\tilde{c}^{\dagger}_{i\downarrow}\tilde{c}_{i\downarrow}=X^{\uparrow\uparrow}_i+X^{\downarrow\downarrow}_i=1-X^{00}_i=1-f^{\dagger}_if_i.
\end{aligned} \quad (2)$$

In sublattice $B=\{\downarrow\}$, the corresponding representation is given by

$$\begin{aligned}
&S^z_j=\tfrac{1}{2}(X^{\uparrow\uparrow}_j-X^{\downarrow\downarrow}_j)=-\tfrac{1}{2}+b^{\dagger}_jb_j+\tfrac{1}{2}g^{\dagger}_jg_j,\\
&S^-_j=X^{\downarrow\uparrow}_j=b_j,\quad S^+_j=X^{\uparrow\downarrow}_j=b^{\dagger}_j(1-b^{\dagger}_jb_j-g^{\dagger}_jg_j),\\
&\tilde{c}_{j\uparrow}=X^{0\uparrow}_j=g^{\dagger}_jb_j,\quad \tilde{c}^{\dagger}_{j\uparrow}=X^{\uparrow 0}_j=g_jb^{\dagger}_j,\\
&\tilde{c}_{j\downarrow}=X^{0\downarrow}_j=g^{\dagger}_j(1-b^{\dagger}_jb_j),\quad \tilde{c}^{\dagger}_{j\downarrow}=X^{\downarrow 0}_j=g_j,\\
&\tilde{c}^{\dagger}_{j\uparrow}\tilde{c}_{j\uparrow}+\tilde{c}^{\dagger}_{j\downarrow}\tilde{c}_{j\downarrow}=X^{\uparrow\uparrow}_j+X^{\downarrow\downarrow}_j=1-X^{00}_j=1-g^{\dagger}_jg_j.
\end{aligned} \quad (3)$$

Thus we have two types of fermions and bosons associated with the A and B sublattices. The Hamiltonian in Eq. (1) expressed in terms of the new variables Eqs. (2) and (3) is

$$\begin{aligned}
&\mathcal{H}\Rightarrow\mathcal{H}_0+\mathcal{H}_1+\mathcal{H}_2,\\
&\mathcal{H}_0=\tfrac{1}{2}J\sum_{\langle i,j\rangle}[a^{\dagger}_ia_i+b^{\dagger}_jb_j+f^{\dagger}_if_i+g^{\dagger}_jg_j],\\
&\mathcal{H}_1=t\sum_{\langle ij\rangle}[f^{\dagger}_ig_j(b^{\dagger}_j+a_i)+\text{H.c.}],\\
&\mathcal{H}_2=-t\sum_{\langle ij\rangle}[f^{\dagger}_ig_jb^{\dagger}_ja^{\dagger}_ia_i+g^{\dagger}_jf_ia^{\dagger}_ib^{\dagger}_jb_j]\\
&\quad-\tfrac{1}{2}J\sum_{\langle i,j\rangle}[n^f_ib^{\dagger}_jb_j+n^g_ja^{\dagger}_ia_i+n^f_in^g_j+2a^{\dagger}_ia_ib^{\dagger}_jb_j].
\end{aligned} \quad (4)$$

Here we have divided the Hamiltonian [Eqs. (4)] into three parts: $\mathcal{H}_0$, consisting of the linear spin-excitation and hole terms: $\mathcal{H}_1$ consisting of the bare hole-magnon interaction term, and $\mathcal{H}_2$, consisting of the nonlinear hole-magnon, static hole-magnon, direct hole-hole, and magnon-magnon interaction terms. The third and fourth terms in $\mathcal{H}_0$ take into account the energy of the four AF bonds broken by a hole introduced into the system. In the following this energy is included in the ground-state energy and the corresponding terms are omitted. Note that we have omitted a constant term. The same Hamiltonian [Eqs. (4)] in $\mathbf{k}$ space is given by

$$\begin{aligned}
&\mathcal{H}_0=2J\sum_{\mathbf{q}}[a^{\dagger}_{\mathbf{q}}a_{\mathbf{q}}+b^{\dagger}_{\mathbf{q}}b_{\mathbf{q}}]+2J\sum_{\mathbf{k}}[f^{\dagger}_{\mathbf{k}}f_{\mathbf{k}}+g^{\dagger}_{\mathbf{k}}g_{\mathbf{k}}],\\
&\mathcal{H}_1=4t\sum_{\mathbf{k},\mathbf{q}}\gamma_{\mathbf{k}-\mathbf{q}}[f^{\dagger}_{\mathbf{k}-\mathbf{q}}g_{\mathbf{k}}b^{\dagger}_{\mathbf{q}}+g^{\dagger}_{\mathbf{k}-\mathbf{q}}f_{\mathbf{k}}a^{\dagger}_{\mathbf{q}}+\text{H.c.}],
\end{aligned} \quad (5)$$

$$\begin{aligned}
\mathcal{H}_2=&-4t\sum_{\mathbf{k},\mathbf{q},\mathbf{q}_1,\mathbf{q}_2}\gamma_{\mathbf{k}-\mathbf{q}}[f^{\dagger}_{\mathbf{k}-\mathbf{q}-\mathbf{q}_1+\mathbf{q}_2}g_{\mathbf{k}}b^{\dagger}_{\mathbf{q}}a^{\dagger}_{\mathbf{q}_1}a_{\mathbf{q}_2}\\
&+g^{\dagger}_{\mathbf{k}-\mathbf{q}-\mathbf{q}_1+\mathbf{q}_2}f_{\mathbf{k}}a^{\dagger}_{\mathbf{q}}b^{\dagger}_{\mathbf{q}_1}b_{\mathbf{q}_2}]\\
&-2J\sum_{\mathbf{k},\mathbf{q},\mathbf{q}_1}\gamma_{\mathbf{q}-\mathbf{q}_1}[f^{\dagger}_{\mathbf{k}-\mathbf{q}+\mathbf{q}_1}f_{\mathbf{k}}b^{\dagger}_{\mathbf{q}}b_{\mathbf{q}_1}+g^{\dagger}_{\mathbf{k}-\mathbf{q}+\mathbf{q}_1}g_{\mathbf{k}}a^{\dagger}_{\mathbf{q}}a_{\mathbf{q}_1}]\\
&-2J\sum_{\mathbf{k},\mathbf{k}',\mathbf{q}}\gamma_{\mathbf{q}}f^{\dagger}_{\mathbf{k}-\mathbf{q}}g^{\dagger}_{\mathbf{k}'+\mathbf{q}}g_{\mathbf{k}'}f_{\mathbf{k}}\\
&-4J\sum_{\mathbf{q}_1,\mathbf{q}_2,\mathbf{q}}\gamma_{\mathbf{q}}a^{\dagger}_{\mathbf{q}_1-\mathbf{q}}b^{\dagger}_{\mathbf{q}_2+\mathbf{q}}b_{\mathbf{q}_2}a_{\mathbf{q}_1},
\end{aligned} \quad (6)$$

where $\gamma_{\mathbf{k}}=[\cos(k_x)+\cos(k_y)]/2$, and all summations are restricted to the first magnetic Brillouin zone (BZ).

III. PROPAGATORS AND VERTEX FUNCTIONS

The Feynman rules for the model in Eq. (5) are as follows.

(i) Hole propagator: $G^0(\epsilon)=G^0_{f(g)}(\epsilon)=[\epsilon+i0]^{-1}$ [Fig. 1(a)].

(ii) Magnon propagator: $D^0(\omega)=D^0_{a(b)}(\omega)=[\omega-2J+i0]^{-1}$ [Fig. 1(b)].

(iii) Hole-magnon vertex: $\Gamma^0(k,q,k-q)=4t\gamma_{\mathbf{k}-\mathbf{q}}\delta_{\epsilon_1,\epsilon-\omega}$ [Fig. 1(c)]. The indices indicate that f (or g) holes can emit only a (or b) magnons and absorb only b (or a) magnons. This is an important feature of the hole-

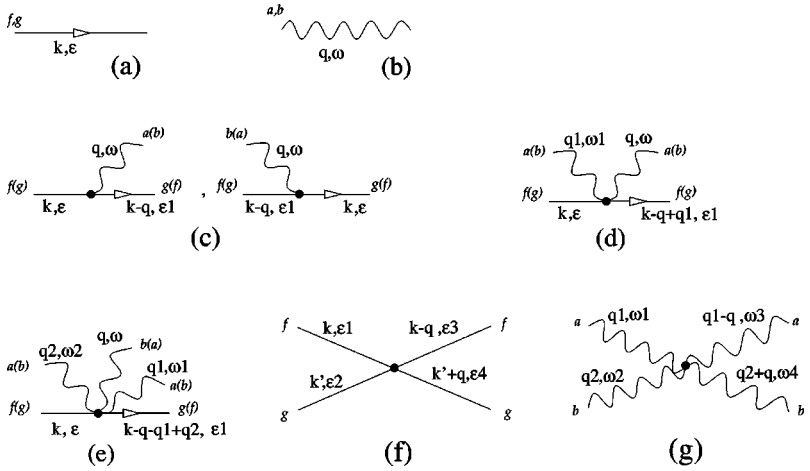

FIG. 1. Feynman rules for Hamiltonian (5).

magnon interaction, and is a consequence of spin conservation. In the following we omit the indices. We use the following shorthand notations: $\delta_{\epsilon_1,\epsilon-\omega}$ denotes $\delta(\epsilon_1-\epsilon+\omega)$, and Σ_ω means $\int_{-\infty}^{\infty}(d\omega/2\pi i)$.

(iv) Hole-two-magnon vertex: $\Gamma_2^0(k,q,q_1,k-q+q_1)=-2J\gamma_{\mathbf{q}-\mathbf{q}_1}\delta_{\epsilon_1,\epsilon-\omega+\omega_1}$ [Fig. 1(d)]. Note that f (or g) holes interact with a (or b) magnons only.

(v) Hole-three-magnon vertex: $\Gamma_3^0(k,q,q_1,q_2,k-q-q_1+q_2)=-4t\gamma_{\mathbf{k}-\mathbf{q}}\delta_{\epsilon_1,\epsilon-\omega-\omega_1+\omega_2}$ [Fig. 1(e)]. Note that there is no vertex diagram for the reversed order of emission-absorption because of the non-Hermitian nature of the corresponding terms in the Hamiltonian [Eq. (5)].

(vi) Hole-hole vertex: $\Gamma_{fg}^0(k,k',q)=-2J\gamma_{\mathbf{q}}\delta_{\epsilon_1+\epsilon_2,\epsilon_3+\epsilon_4}$ [Fig. 1(f)].

(vii) Magnon-magnon vertex: $\Gamma_{ab}^0(q_1,q_2,q)=-4J\gamma_{\mathbf{q}}\delta_{\omega_1+\omega_2,\omega_3+\omega_4}$ [Fig. 1(g)].

In all cases we use the notations $k=(\mathbf{k},\epsilon)$ and $q=(\mathbf{q},\omega)$ for the momentum and frequency of the hole and magnon, respectively. Thus the model [Eq. (5)] involves fermion-fermion (hole-hole), boson-boson (magnon-magnon), and three types of fermion-boson (hole-magnon) interactions. In general the problem of finding the low-energy excitations in such a model is very complicated. However, as we will show below, in the case of the t-J_z model it is possible to take into account the result of renormalization almost exactly using a regular diagrammatic treatment.

IV. SINGLE HOLE

If we ignore $\mathcal{H}_2$, the Hamiltonian in Eq. (5) for a system with a single hole is similar to the problem of a single electron interacting with the local phonon mode. When the interaction (t in our case) is small compared to the energy of the boson ($2J$), we can use perturbation theory and consider only the lowest contribution to the hole energy, which corresponds to the virtual emission and absorption of a single magnon. At larger t many-magnon intermediate states must be considered. Such a problem, if solved self-consistently, must take into account the renormalization of the fermion-boson interaction, or crossing diagrams. However, in the t-J model it is well known that the lowest correction to the bare hole-magnon vertex Γ^0 is exactly zero, since the hole-magnon interaction conserves the spin, or more exactly, the pseudospin associated with the sublattice type. Therefore, the crossing diagrams can be omitted and the renormalization of the hole energy is given only by the series of diagrams where the magnons are absorbed in exactly the reversed order in which they are emitted. This is the so-called self-consistent Born approximation (SCBA), which in the case of the t-J_z model is identical to the retraceable path approximation. This coincidence is due to the local nature of the spin excitations in the model. The corresponding diagrammatic equation for the hole Green's function is shown in Fig. 2. Note that the vertices are unrenormalized. The retraceable path approximation implies that the hole is confined by a ''string'' of spin excitations and the hole motion is completely incoherent, i.e., the hole forms a localized state.

The first nonzero contribution to the hole self-energy from the crossing diagrams is shown in Fig. 3. It is of sixth order in t, and is small compared to the contribution of the ''retraceable'' diagrams of the same (sixth) order due to the geometrical factor. This diagram is the first member of the family of the so-called ''Trugman paths.'' Their contribution to the hole energy is small in a wide range of t/J, but they are responsible for the finite coherent band of the hole. Real-space consideration shows that such a diagram corresponds to the hole's motion around an elementary square loop in which the hole makes one and a half turns. As a result all spin excitations are cured, and the hole is translated along the diagonal of the square plaquette, i.e., to a next-nearest neighbor. As we have noted, the corresponding correction to the energy is small, and we will neglect these diagrams in the rest of this section.

Since $G^0(\epsilon)$ and $D^0(\omega)$ are momentum independent and the hole-magnon interaction depends only on $\mathbf{k}-\mathbf{q}$, the full Green's function G is also $\mathbf{k}$ independent. Thus the equation shown in Fig. 2 can be simplified as

$$\Sigma(\epsilon)=\sum_\omega G(\epsilon-\omega)D^0(\omega)\sum_{\mathbf{q}}(\Gamma^0_{\mathbf{k}-\mathbf{q}})^2$$
$$=4t^2G(\epsilon-2J), \tag{7}$$
$$G(\epsilon)=[\epsilon-4t^2G(\epsilon-2J)]^{-1}.$$

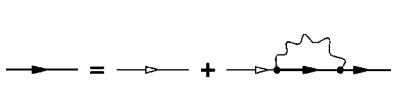

FIG. 2. SCBA for the hole self-energy. Bold lines represent the dressed Green's functions.

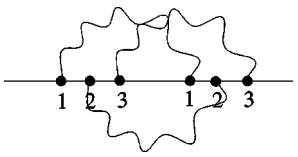

FIG. 3. Trugman's diagram. The numbers represent the sites where a magnon is emitted (absorbed).

The solution of Eq. (7) at all t/J can be found in Ref. 18. One can try an ansatz for G of the form

$$G(\epsilon) = -\frac{1}{2t}\frac{Y(\epsilon)}{Y(\epsilon+2J)}. \tag{8}$$

This transforms Eq. (7) into a difference equation

$$Y(\epsilon+2J)+Y(\epsilon-2J) = -\frac{\epsilon}{2t}Y(\epsilon), \tag{9}$$

which is the recursion relation for the Bessel functions. Thus $G(\epsilon)$ is given by

$$G(\epsilon) = -\frac{1}{2t}\frac{J_{-\epsilon/2J}(2t/J)}{J_{-\epsilon/2J-1}(2t/J)}, \tag{10}$$

where $J_\nu(x)$ are the Bessel functions.

Such a form is the consequence of the continued fraction form of the Green's function, which in turn is the result of the retraceable-path approximation. Note that in Ref. 18, $J_z = 2J$. Thus the poles of the Green's function in the SCBA approximation are defined by the zeros of the Bessel function. Since all these zeros are real, the hole spectral function consists of the set of δ-function peaks corresponding to the energy levels of the quasiparticle states in the ''string'' potential well. Inclusion of the Trugman processes does not change this result significantly, because the resulting bandwidth is much smaller than the separation of the levels.

Although the solution [Eq. (10)] of Eq. (7) is an almost exact solution of $\mathcal{H}_0+\mathcal{H}_1$, it is not a solution of the original t-J_z Hamiltonian. Besides the crossing diagrams, there are other contributions to the self-energy originating from $\mathcal{H}_2$. In order to compare with other analytical approaches and ED, it is necessary to account for these contributions. To make this statement evident let us now consider the two limiting cases $t/J \ll 1$ and $t/J \gg 1$, and compare the results of the SCBA with the known facts from the real-space approach and ED numerical data.

For $t/J \ll 1$ the ground-state energy for the hole is given by Eqs. (7) as

$$\epsilon_0^{SCBA} = -\frac{2t^2}{J}. \tag{11}$$

This is inconsistent with the result of the real-space approach

$$\epsilon_0 = -\frac{8t^2}{3J}. \tag{12}$$

The reason for this discrepancy is that the spin-flip (magnon) has lower energy ($3J/2$ compared to $2J$) if it is located in the neighborhood of the hole, and the Hamiltonian $\mathcal{H}_0+\mathcal{H}_1$ does not take this difference into account. Note that throughout this paper we assign the zero energy level to the state with one *static* hole, i.e., $E_0 = E_0^{Ising} + 2J = 0$.

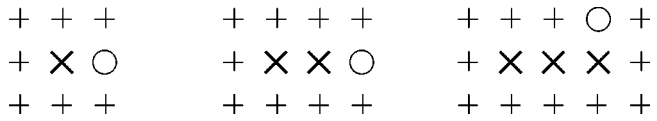

FIG. 4. One-, two-, and three-magnon strings.

According to Ref. 18, in the large-t limit the ground-state energy given by Eq. (10) is

$$\epsilon_0^{SCBA} = -4t + 2\beta_0 t(J/t)^{2/3} - 2J \ , \tag{13}$$

where $\beta_0 = 2.34$ is the first zero of the Airy function. There is no alternative asymptotic expression in this limit which is accurate up to order J, but the first two terms which are of order t and $t^{1/3}J^{2/3}$ can be compared to the results of the ''string'' approach by Shraiman and Siggia[20] (SS) and the fitting of 16-site ED data by Barnes *et al.*:[23]

$$\begin{aligned} \epsilon_0^{SS} &= -2\sqrt{3}t + 2.74t(J/t)^{2/3}, \\ \epsilon_0^{ED} &= -3.63t + 2.93t(J/t)^{2/3}. \end{aligned} \tag{14}$$

This comparison makes one suspect that the SCBA [Eq. (13)] overestimates both the absolute value of the depth of the ''band'' and the slope of the walls of the linear confining potential.

The origin of these discrepancies becomes evident when we consider the real-space picture of the retraceable hole movement. Figure 4 shows the real-space images of three components of the spin-polaron wave function: the one-, two-, and three-magnon strings. The first important observation is that the coordination number in the creation of the first magnon is indeed $z=4$, but is $z-1=3$ in the creation of each next magnon. This is why the factor in the first term of the SS expression [Eq. (14)] for the hole energy is $2\sqrt{3}$ (instead of 4). If t is much larger than J, the average length of the strings contributing to the spin-polaron wave function is large. Then the weight of the components with coordination number different from others becomes insignificant. Since this component is the ''bare'' hole, it also means that the quasiparticle residue of the state decreases as t grows, and in the $t\to\infty$ limit the spectrum will be incoherent. This result was first obtained by Brinkmann and Rice[11] in the $J=0$ limit.

Keeping in mind that the energy of spin excitation is determined by the number of broken AF bonds associated with its creation, one can see that the energy of the first magnon in the string is $3J/2$ (three bonds, $J/2$ each), but the energy of each subsequent magnon is just J (two bonds). This is true for all strings of length $l=2$ and for most other longer strings except for those which have self-tangencies. Since the latter cases are relatively rare due to the geometrical factor, one can assign the same energy $lJ+J/2$ to every string of length l. A more accurate account for the energy of the self-tangent strings makes only tiny changes in the energy of the whole excitation. Thus making the changes $2J\to J$ and $z\to z-1$ in the expression for the SCBA hole energy will change the factor $2\beta_0 = 4.68$ in the second term of Eq. (13) to $3^{1/6}\beta_0 = 2.81$, leaving it in reasonable agreement with Eq. (14).

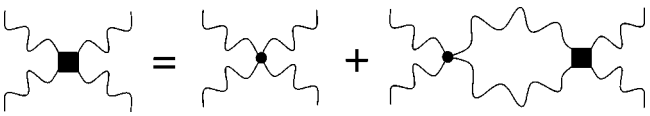

FIG. 5. The Bethe-Salpeter equation for the two-magnon problem. Dots represent bare vertices Γ^0_{ab}, and squares represent full vertices Γ_{ab}.

Summarizing the results of the comparison, one can say that the reason for the failure of the SCBA is that $\mathcal{H}_0+\mathcal{H}_1$ is not the same as $\mathcal{H}_{t-J}$, and that an improved formalism must take into account the following facts: (i) the energy of the first magnon in a string is $3J/2$; (ii) the energy of the nth magnon ($n>1$) is J; (iii) the coordination number is $z-1=3$ for $l\geqslant 1$ and $z=4$ for $l=0$, where l is the length of the string. After some thinking using the above real-space arguments, one can suggest the following modification to the equation for the Green's function [Eq. (7)] to meet all these requirements:

$$G(\epsilon)=[\epsilon-4t^2G_a(\epsilon-3J/2)]^{-1},$$
$$G_a(\epsilon)=[\epsilon-3t^2G_a(\epsilon-J)]^{-1}, \tag{15}$$
$$G_a(\epsilon)=-\frac{1}{\sqrt{3}t}\frac{J_{-\epsilon/J}(2\sqrt{3}t/J)}{J_{-\epsilon/J-1}(2\sqrt{3}t/J)}.$$

Such a modification gives the correct hole energy in the small-t limit. In the $t\to\infty$ limit the resulting hole energy is $-2\sqrt{3}t$.

Let us now come back to the original problem with the full Hamiltonian $\mathcal{H}_0+\mathcal{H}_1+\mathcal{H}_2$, [Eq. (5)], and discuss how such an ''improvement'' of the Green's function proposed in Eqs. (15) can be done formally in the diagrammatic language. The fact that magnons in the string have lower energy than free excitations is the result of magnon-magnon binding. The magnon-magnon interaction [last term of $\mathcal{H}_2$, Eq. (5)] is attractive and leads to a bound state. A regular approach to the bound-state problem is based on the Bethe-Salpeter equation shown in Fig. 5. The equivalent integral equation is

$$\Gamma_{ab}(\Omega,\mathbf{q}_1-\mathbf{q}_3)=\Gamma^0_{ab}(\mathbf{q}_1-\mathbf{q}_3)+\sum_{\mathbf{p}_1}\Gamma^0_{ab}(\mathbf{q}_1-\mathbf{p}_1)\times\Gamma_{ab}(\Omega,\mathbf{p}_1-\mathbf{q}_3)\sum_{\omega}D^0(\omega)D^0(\Omega-\omega)$$
$$=-4J\gamma_{\mathbf{q}_1-\mathbf{q}_3}+\sum_{\mathbf{p}_1}(-4J\gamma_{\mathbf{q}_1-\mathbf{p}_1})\times\frac{\Gamma_{ab}(\Omega,\mathbf{p}_1-\mathbf{q}_3)}{\Omega-4J+i0}. \tag{16}$$

It is easy to see that the momentum and frequency dependence of the vertex can be separated. The suggestion $\Gamma_{ab}(\Omega,\mathbf{q}_1-\mathbf{q}_3)=-4J\gamma_{\mathbf{q}_1-\mathbf{q}_3}\tilde{\Gamma}_{ab}(\Omega)$ transforms Eq. (16) into

$$\tilde{\Gamma}_{ab}(\Omega)=1-\frac{J}{\Omega-4J+i0}\tilde{\Gamma}_{ab}(\Omega). \tag{17}$$

Here we have used the relation $\Sigma_{\mathbf{p}_1}\gamma_{\mathbf{q}_1-\mathbf{p}_1}\gamma_{\mathbf{p}_1-\mathbf{q}_3}=\gamma_{\mathbf{q}_1-\mathbf{q}_3}/4$. Thus the renormalized magnon-magnon vertex is given by

$$\Gamma_{ab}(\Omega,\mathbf{k}-\mathbf{p})=-4J\gamma_{\mathbf{k}-\mathbf{p}}\frac{\Omega-4J+i0}{\Omega-3J+i0}. \tag{18}$$

The pole of this function, $\Omega=3J$, corresponds to the bound state whose energy is lower than that of two free magnons by $-J$, in agreement with our expectations.

Similarly the hole–two-magnon interaction [the second term in $\mathcal{H}_2$, Eq. (5)] lowers the energy of the magnons in the neighborhood of a hole. The hole–three-magnon interaction (first term in $\mathcal{H}_2$) originates from the projection operator and projects out the unphysical states with the hole and magnon at the same site created by the hopping term in $\mathcal{H}_0$. A consistent consideration of these interactions yields the following Dyson equation for the single-hole propagator:

$$G(\epsilon)=[\epsilon-\Sigma(\epsilon)]^{-1},$$
$$\Sigma(\epsilon)=\sum_{\omega}G(\epsilon-\omega)D^0(\omega)\sum_{\mathbf{q}}\Gamma^0_{\mathbf{k}-\mathbf{q}}\Gamma_{\mathbf{k},\mathbf{q}}(\epsilon,\omega), \tag{19}$$

where the renormalized hole-magnon vertex is

$$\Gamma_{\mathbf{k},\mathbf{q}}(\epsilon,\omega)=\Gamma^0_{\mathbf{k}-\mathbf{q}}+\Gamma^{(1)}_{\mathbf{k},\mathbf{q}}(\epsilon)+\Gamma^{(2)}_{\mathbf{k},\mathbf{q}}(\epsilon,\omega)+\Gamma^{(3)}_{\mathbf{k},\mathbf{q}}(\epsilon)+\Gamma^{(4)}_{\mathbf{k},\mathbf{q}}(\epsilon),$$

$$\Gamma^{(1)}_{\mathbf{k},\mathbf{q}}(\epsilon)=\sum_{\mathbf{q}_1,\omega_1}\Gamma^0_2(\mathbf{q}-\mathbf{q}_1)G(\epsilon-\omega_1)D^0(\omega_1)\Gamma_{\mathbf{k},\mathbf{q}_1}(\epsilon,\omega_1),$$

$$\Gamma^{(2)}_{\mathbf{k},\mathbf{q}}(\epsilon,\omega)=\sum_{\mathbf{q}_1,\mathbf{q}_2}\sum_{\omega_2,\Omega}\Gamma^0_{\mathbf{k}-\mathbf{q}-\mathbf{q}_1}D^0(\Omega-\omega)\times G(\epsilon-\Omega)\Gamma_{ab}(\Omega,\mathbf{k}-\mathbf{q}_2)D^0(\omega_2)D^0(\Omega-\omega_2)\times G(\epsilon-\omega_2)\Gamma_{\mathbf{k},\mathbf{q}+\mathbf{q}_1}(\epsilon-\omega_2,\Omega-\omega_2)\times\Gamma_{\mathbf{k},\mathbf{q}_2}(\epsilon,\omega_2), \tag{20}$$

$$\Gamma^{(3)}_{\mathbf{k},\mathbf{q}}(\epsilon)=\sum_{\mathbf{q}_1,\mathbf{q}_2}\sum_{\omega_1,\omega_2}\Gamma^0_3(\mathbf{k}-\mathbf{q}-\mathbf{q}_2)D^0(\omega_1)D^0(\omega_2)\times G(\epsilon-\omega_1-\omega_2)\Gamma_{\mathbf{k}-\mathbf{q}-\mathbf{q}_2}(\epsilon-\omega_1,\omega_2)\times G(\epsilon-\omega_1)\Gamma_{\mathbf{k},\mathbf{q}_1}(\epsilon,\omega_1),$$

$$\Gamma^{(4)}_{\mathbf{k},\mathbf{q}}(\epsilon)=\sum_{\mathbf{q}_1,\mathbf{q}_2,\mathbf{Q}}\sum_{\omega_1,\omega_2,\Omega}\Gamma^0_3(\mathbf{k}-\mathbf{q}-\mathbf{Q})D^0(\omega_1)\times D^0(\Omega-\omega_1)G(\epsilon-\Omega)\Gamma_{ab}(\Omega,\mathbf{q}_1-\mathbf{q}_2)\times D^0(\omega_2)D^0(\Omega-\omega_2)\Gamma_{\mathbf{k},\mathbf{q}_1+\mathbf{Q}}(\epsilon-\omega_2,\Omega-\omega_2)\times G(\epsilon-\omega_2)\Gamma_{\mathbf{k},\mathbf{q}_2}(\epsilon,\omega_2).$$

A diagrammatic representation of Eqs. (19) and (20) is shown in Fig. 6.

Note that the lowest-order correction to *all* vertices are zero, and higher-order corrections are neglected. We have already discussed the absence of one-loop correction to the hole-magnon vertex. It is less evident in cases of the hole–

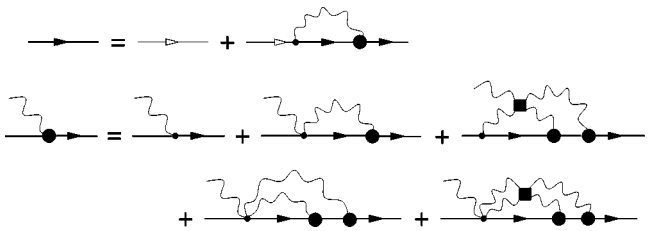

FIG. 6. The Dyson equation for the hole Green's function. Bold lines are the dressed Green's functions, circles are the renormalized hole-magnon vertices, and squares are the renormalized magnon-magnon vertices [Fig. 5 and Eq. (18)].

two-magnon and hole–three-magnon vertices. However, if one recalls the f,g and a,b indices for the hole and magnon lines in Fig. 6, it becomes evident that the emission of an extra magnon prior to the hole–two-magnon interaction alters the type of the hole, and therefore prevents it from absorbing and reemitting the original magnon. The same is true for the hole–three-magnon vertex. It is interesting to note that the set of diagrams in Fig. 6 is still in the SCBA, i.e., the crossing diagrams are absent.

Again the momentum and frequency dependence of Γ can be separated. The almost evident substitution $\Gamma_{\mathbf{k},\mathbf{q}}(\epsilon,\omega) = 4t\gamma_{\mathbf{k}-\mathbf{q}}\tilde{\Gamma}(\epsilon,\omega)$ simplifies Eqs. (19) and (20) which, after integrating over the internal frequencies and momenta, become

$$\Sigma(\epsilon) = 4t^2 G(\epsilon-2J)\tilde{\Gamma}(\epsilon,2J), \tag{21}$$

$$\begin{aligned}\tilde{\Gamma}(\epsilon,\omega) = 1 - G(\epsilon-2J)\tilde{\Gamma}(\epsilon,2J)\Bigg[&\frac{J}{2} - 4t^2\frac{J}{\omega-J}\\ &\times[G(\epsilon-3J)\tilde{\Gamma}(\epsilon-2J,J) - G(\epsilon-2J-\omega)\\ &\times\tilde{\Gamma}(\epsilon-2J,\omega)] + t^2 G(\epsilon-4J)\tilde{\Gamma}(\epsilon-2J,2J)\\ &+ t^2[G(\epsilon-3J)\tilde{\Gamma}(\epsilon-2J,J) - G(\epsilon-4J)\\ &\times\tilde{\Gamma}(\epsilon-2J,2J)]\Bigg].\end{aligned}$$

Each term in the square brackets comes from the corresponding irreducible diagram in Fig. 6. After combining similar terms $\tilde{\Gamma}(\epsilon,2J)$ becomes

$$\begin{aligned}\tilde{\Gamma}(\epsilon,2J) &= G(\epsilon-2J)^{-1}[G(\epsilon-2J)^{-1} + J/2\\ &\quad - 3t^2 G(\epsilon-3J)\tilde{\Gamma}(\epsilon-2J,J) + 4t^2 G(\epsilon-4J)\\ &\quad \times\tilde{\Gamma}(\epsilon-2J,2J)]^{-1}\\ &= G(\epsilon-2J)^{-1}[\epsilon - 3J/2 - 3t^2 G(\epsilon-3J)\\ &\quad \times\tilde{\Gamma}(\epsilon-2J,J)]^{-1}\\ &= \frac{G_a(\epsilon-3J/2)}{G(\epsilon-2J)},\end{aligned} \tag{22}$$

where $G_a(\epsilon)$ has a continued fraction form. Summarizing Eqs. (19), (21), and (22), one finally obtains

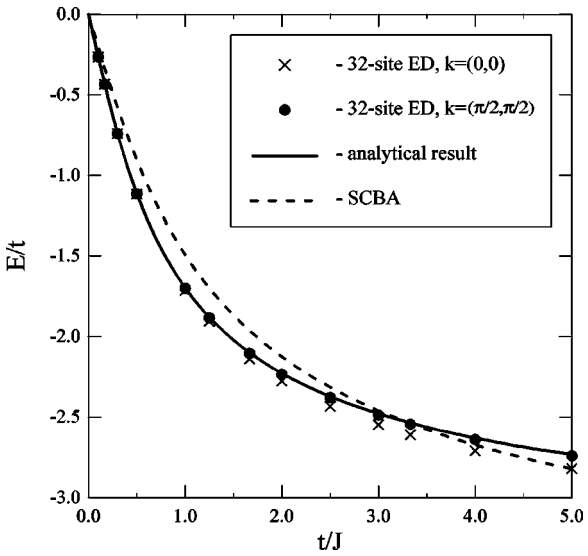

FIG. 7. The single-hole ground-state energy vs t/J. The zero level of energy is taken to be the energy of the hole at $t=0$.

$$G(\epsilon) = [\epsilon - 4t^2 G_a(\epsilon - 3J/2)]^{-1},$$

$$G_a(\epsilon) = [\epsilon - 3t^2 G_a(\epsilon - J)]^{-1} = -\frac{1}{\sqrt{3}t}\frac{J_{-\epsilon/J}(2\sqrt{3}t/J)}{J_{-\epsilon/J-1}(2\sqrt{3}t/J)}, \tag{23}$$

which is exactly the same as the Green's function suggested in Eq. (15).

The rest of this section is devoted to the comparison of the results from Eq. (23) with our numerical ED results on a 32-site lattice. Figure 7 shows the ED results together with analytical results from the SCBA [Eq. (7)] and from Eq. (23). We recall that contributions from the Trugman's paths are left out from Eqs. (23) and (7). These paths give rise to a small dispersion of the hole, $\delta E_{\mathbf{k}} = t_1^{eff}\cos(k_x)\cos(k_y) + t_2^{eff}[\cos(2k_x)+\cos(2k_x)]+\cdots$, with $t_2^{eff} \ll t_1^{eff}$. This form of dispersion implies that the correction to the energy at the point $(\pi/2,\pi/2)$ due to the Trugman paths is almost zero. Therefore, it is natural to compare the ED data at this $\mathbf{k}$ point to the analytical results. From Fig. 7 one can see a beautiful agreement of the numerical data at $\mathbf{k}=(\pi/2,\pi/2)$ with the results of Eq. (23) in the whole range of t/J. For comparison purposes, Fig. 7 also shows the numerical data at $\mathbf{k}=(0,0)$. We also remark that our 32-site ED data at $\mathbf{k}=(0,0)$ agree with the 50-site results of the modified Lanczos study by Riera and Dagotto[24] (not shown in Fig. 7) up to the fourth digit at $t/J=5$ and up to the seventh digit at $t/J=1.25$.

It is already clear from Fig. 7 that our present approach works better than the SCBA. To illustrate this point further, we plot the quasiparticle residue in Fig. 8. Three sets of data are shown. They are the results from our present analytical approach, the SCBA, and our numerical ED study. The ED results are calculated using the same method as in Ref. 26. One can see that such a comparison unambiguously favors the present approach.

V. TWO HOLES

In this section we consider the problem of hole pairing in the t-J_z model using the diagrammatic formalism introduced

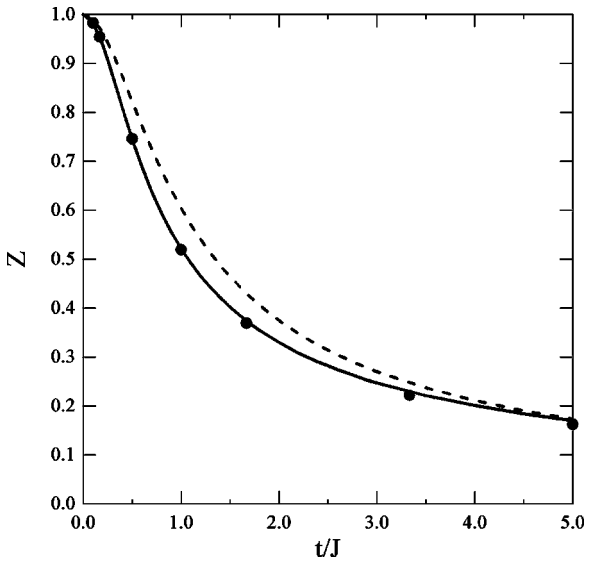

FIG. 8. Quasiparticle residue for the lowest pole vs t/J. The dashed curve is the result of the SCBA. The solid curve is the result of the present approach. Dots are the numerical data for the $(\pi/2,\pi/2)$ point.

in previous sections. Our goal is to study in detail the bound state of two holes. The role of different interactions and higher-order corrections will be analyzed. Bound states with *s*, *p*, and *d* symmetries and zero total momentum will be investigated. Throughout this paper we consider the $S^z=0$ bound states only. Consequently we are interested in the interactions of the particles originating from different sublattices (f and g fermions).

If an exact two-particle Green's function has a pole in the scattering channel at a fixed total energy of the particles, then there exists a bound state whose energy is the total energy of the particles. Thus to analyze the bound-state problem of two holes one has to solve the Bethe-Salpeter (BS) equation, whose most general form is given by

$$\hat{\Gamma}^{fg}_{\mathbf{P},\mathbf{k},\mathbf{p}}(\Omega,\epsilon,\epsilon')=\Gamma^{fg}_{\mathbf{P},\mathbf{k},\mathbf{p}}(\Omega,\epsilon,\epsilon')+\sum_{\mathbf{p}_1,\epsilon_1}\Gamma^{fg}_{\mathbf{P},\mathbf{k},\mathbf{p}_1}(\Omega,\epsilon,\epsilon_1)\times G_{\mathbf{P/2}+\mathbf{p}_1}(\Omega/2+\epsilon_1)G_{\mathbf{P/2}-\mathbf{p}_1}(\Omega/2-\epsilon_1)\times\hat{\Gamma}^{fg}_{\mathbf{P},\mathbf{p}_1,\mathbf{p}}(\Omega,\epsilon_1,\epsilon'), \tag{24}$$

where

$$\mathbf{P}=\mathbf{k}_1+\mathbf{k}_2=\mathbf{k}_3+\mathbf{k}_4=\mathbf{k}_{1'}+\mathbf{k}_{2'},\quad \mathbf{k}=(\mathbf{k}_1-\mathbf{k}_2)/2,$$
$$\mathbf{p}=(\mathbf{k}_3-\mathbf{k}_4)/2,\quad \mathbf{p}_1=(\mathbf{k}_{1'}-\mathbf{k}_{2'})/2,$$
$$\Omega=\epsilon_1+\epsilon_2=\epsilon_3+\epsilon_4=\epsilon_{1'}+\epsilon_{2'},\quad \epsilon=(\epsilon_1-\epsilon_2)/2,$$
$$\epsilon'=(\epsilon_3-\epsilon_4)/2,\quad \epsilon_1=(\epsilon_{1'}-\epsilon_{2'})/2, \tag{25}$$

and the indices are given in accordance with Fig. 9.

The bare vertex function Γ^{fg} includes all diagrams which cannot be reduced to the second term of Eq. (24), i.e., those which cannot be cut by a vertical line between the ends 1,2 and 3,4 into two parts joined only by two hole lines. The set of all such diagrams is called a ''compact'' vertex.

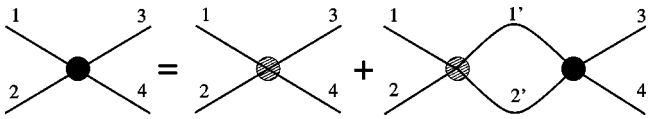

FIG. 9. The Bethe-Salpeter equation for the two-hole problem. Lines represent renormalized Green's functions, dashed circles represent the bare ''compact'' vertex function Γ^{fg}, and black circles represent the exact vertex $\hat{\Gamma}^{fg}$.

At the pole, when $\Omega=E$ (E is the energy of the bound state), the left-hand side and the second term on the right-hand side of Eq. (24) are singular. Therefore $\hat{\Gamma}^{fg}\gg\Gamma^{fg}$, and the first term on the right-hand side can be neglected. Hence the integral equation (24) becomes homogeneous in $\hat{\Gamma}^{fg}$. The variables $\mathbf{p}$ and ϵ' become parameters and are not defined by the equation itself. Omitting them and the indices f and g yields

$$\hat{\Gamma}_{\mathbf{P},\mathbf{k}}(E,\epsilon)=\sum_{\mathbf{p}_1,\epsilon_1}\Gamma_{\mathbf{P},\mathbf{k},\mathbf{p}_1}(E,\epsilon,\epsilon_1)G_{\mathbf{P/2}+\mathbf{p}_1}(E/2+\epsilon_1)\times G_{\mathbf{P/2}-\mathbf{p}_1}(E/2-\epsilon_1)\hat{\Gamma}_{\mathbf{P},\mathbf{p}_1}(E,\epsilon_1). \tag{26}$$

Further simplifications of this general formula (26) are possible based on the specifics of the problem being considered. Rather general and frequently used simplifications can be performed, for example, when the bare interaction Γ is a potential-like term, i.e., independent of the frequency. In this case $\hat{\Gamma}$ becomes ϵ independent and plays only an auxiliary role. Furthermore, it is more convenient to use the bound-state wave function $\psi_{\mathbf{P},\mathbf{k}}(E)=\Sigma_\epsilon GG\hat{\Gamma}$. By changing the variables and integrating both sides of Eq. (26) over ϵ, we obtain the Schrödinger equation for the bound state in the momentum representation:

$$\psi_{\mathbf{P},\mathbf{k}}(E)=\left(\sum_{\epsilon}G_{\mathbf{P/2}+\mathbf{k}}(E/2+\epsilon)G_{\mathbf{P/2}-\mathbf{k}}(E/2-\epsilon)\right)\times\sum_{\mathbf{p}_1}\Gamma_{\mathbf{P},\mathbf{k},\mathbf{p}_1}\psi_{\mathbf{P},\mathbf{p}_1}(E). \tag{27}$$

If the Green's functions are the bare ones, the sum over ϵ simply gives $1/[E-\epsilon(\mathbf{P/2}+\mathbf{k})-\epsilon(\mathbf{P/2}-\mathbf{k})]$, where $\epsilon(\mathbf{k})$ is the single-particle energy. In the t-J_z model the following characteristics allow one to simplify Eq. (26) considerably, and obtain most of the results for the bound-state problem in a transparent analytical form:

(i) The single-hole Green's function is mostly $\mathbf{k}$ independent, meaning that in a wide range of t/J ratio the $\mathbf{k}$-dependent contribution to the self-energy is insignificant or small.

(ii) The lowest-order contributions to the compact vertex $\Gamma_{\mathbf{P},\mathbf{k},\mathbf{p}_1}(E,\epsilon,\epsilon_1)$ have a simple kinematic structure and, together with (i), allow one to separate the momentum and frequency dependence of the exact vertex $\hat{\Gamma}$. Its $\mathbf{k}$-dependent part can be classified in terms of *s*-, *p*-, and *d*-wave harmonics and can be integrated out easily.

(iii) All one-loop and lowest-order crossing corrections are exactly zero because of spin conservation in the hole-magnon interaction. Nonzero corrections are of higher order

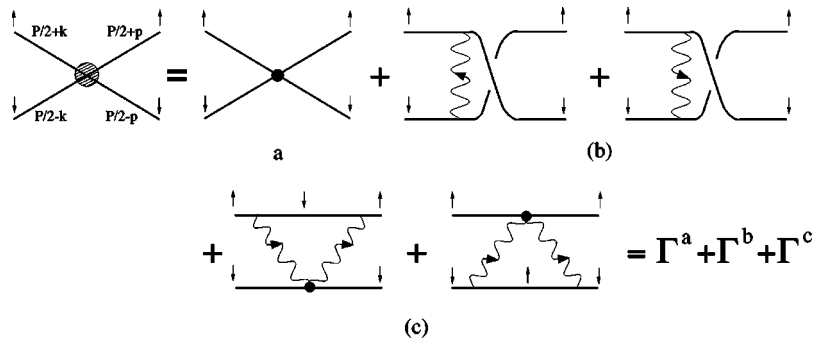

FIG. 10. The lowest-order diagrams contributing to the ''compact'' vertex function Γ: (a) is due to nearest-neighbor hole-hole attraction, (b) are the one-magnon-exchange diagrams, and (c) are the two-magnon exchange diagrams. (a), (b), and (c) are of first, second, and third orders in $\mathcal{H}_{int}$, respectively. Since the emission of magnon changes the spin of the hole, the positions of the ends of the lines in the diagrams in (b) are interchanged. $P/2\pm k=(\mathbf{P}/2\pm\mathbf{k},E/2\pm\epsilon)$ and $P/2\pm p=(\mathbf{P}/2\pm\mathbf{p},E/2\pm\epsilon_1)$.

and are expected to be small. Therefore, the lowest-order diagrams in Γ can be left unrenormalized.

(iv) As we have shown in Sec. III the single-hole spectral function consists of a set of well separated quasiparticle peaks. Therefore, the Green's function of the hole can always be written in the form

$$G(\epsilon)=\sum_{\nu}\frac{a_\nu}{\epsilon-\epsilon_\nu+i0}, \tag{28}$$

where a_ν and ϵ_ν are the residue and the energy of the pole ν, respectively. Then, if the characteristic binding energy is much smaller than the separation between the quasiparticle peaks ($\Delta=E-2\epsilon_0\ll\delta\epsilon$), i.e., one-half of the bound-state energy is close to the lowest peak ($E/2\approx\epsilon_0$), one can safely neglect the contribution of the higher poles and use the lowest-pole approximation for the hole Green's function:

$$G(\epsilon)\approx\frac{a_0}{\epsilon-\epsilon_0+i0}. \tag{29}$$

As a matter of fact, in the limiting case $t\gg J$ the separation of the levels is $\delta\epsilon\sim J(t/J)^{1/3}$, whereas the binding energy, as we will show, is $\Delta\sim -J(J/t)$. Thus $\Delta/\delta\epsilon\sim(J/t)^{4/3}\ll 1$, and the lowest-pole approximation should work well. In the opposite limit $t\ll J$ the binding energy is $\Delta\sim -J/2$ while the separation of the quasiparticle poles is $\delta\epsilon\sim 2J$. Besides a factor of the order of $\Delta/\delta\epsilon\sim 1/4$, the contribution of the higher poles is strongly reduced because their quasiparticle residues are negligible ($\sim t^2/J^2$), thus justifying the lowest-pole approximation in this case. One can then argue that the same is true for all t/J.

With these ideas in mind let us look at the compact vertex Γ. The lowest order contributions to the hole-hole compact vertex Γ are given in Fig. 10. Γ^a, Γ^b, and Γ^c are of first, second, and third orders in $\mathcal{H}_{int}=\mathcal{H}_1+\mathcal{H}_2$ [Eq. (4)], respectively. They can also be classified in terms of powers of J and t: $\Gamma^a\sim J$, $\Gamma^b\sim t^2/J$, and $\Gamma^c\sim t^2/J$.

If we consider Γ^b only, the full vertex $\hat{\Gamma}$ in Fig. 9 is given by the sum of the ladder diagrams only. To some extent, this approximation is analogous to the SCBA in the single-hole problem, and possesses an important property of the latter: all crossing diagrams and one-loop corrections are exactly zero. More importantly, such corrections to *all* the lowest-order diagrams (Γ^a, Γ^b, and Γ^c) are also zero because of the same spin-conservation rule. For the same reason, higher-order corrections to Fig. 10 are strongly suppressed, so that the first dressing of Γ^a, Γ^b, and Γ^c by magnons appears in the fifth, sixth, and seventh orders, respectively. The corresponding set of diagrams is given in Fig. 11. Note that because all these corrections are of similar origin to the Trugman's processes for the self-energy, one can expect that they play only a minor role in the effective interaction.

However, there are other sources of correction to Γ coming from the hole–two-magnon, hole–three-magnon, and magnon-magnon interactions. Most of them result in the renormalization of the hole-magnon vertices similar to those in Fig. 6. While a formal account of such corrections is rather difficult, one can anticipate the result of such a renormalization using the real-space consideration of the interactions. As in the single-hole case, the dressing of the vertex accounts for two facts. First, the energy of a magnon in the neighborhood of a hole is $-J/2$ per hole-magnon link lower than the energy of a free excitation. Second, the coordination number for hole hopping in a state with a string of magnons is $z-1$ instead of z. The first effect renormalizes the energy of the magnon lines in Γ^b and Γ^c, while the second effect renormalizes the inner hole line in Γ^c. In what follows we will consider the compact vertex Γ as given by $\Gamma^a+\Gamma^b+\Gamma^c$ in Fig. 10, and will include the renormalization later.

We first consider the $t=0$ limit when the solution of the BS equation (26) is trivial. In this limit only $\Gamma^a=-2J\gamma_{\mathbf{k}_1-\mathbf{k}_3}$ survives and the hole Green's function is simply $1/\omega$. Thus Eq. (26) becomes

$$\hat{\Gamma}_{\mathbf{P},\mathbf{k}}(E,\epsilon)=-2J\sum_{\mathbf{p}_1}\gamma_{\mathbf{k}-\mathbf{p}_1}\times\sum_{\epsilon_1}\frac{\hat{\Gamma}_{\mathbf{P},\mathbf{p}_1}(E,\epsilon_1)}{(E/2+\epsilon_1+i0)(E/2-\epsilon_1+i0)}. \tag{30}$$

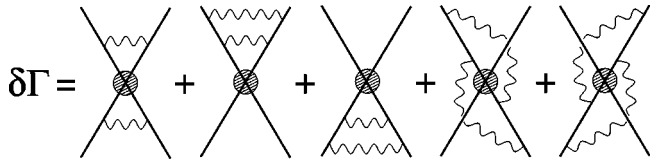

FIG. 11. Lowest-order corrections to the ''compact'' vertex function Γ (Fig. 10). Circles represent $\Gamma=\Gamma^a+\Gamma^b+\Gamma^c$, wavy lines are magnons.

Evidently, the dependence of $\hat{\Gamma}$ on $\mathbf{P}$ is arbitrary and $\hat{\Gamma}(\epsilon)$ is a constant. Integrating over ϵ_1 one finds

$$\hat{\Gamma}_{\mathbf{k}}(E) = -\frac{2J}{E}\sum_{\mathbf{p}_1} \gamma_{\mathbf{k}-\mathbf{p}_1}\hat{\Gamma}_{\mathbf{p}_1}(E), \tag{31}$$

where $\hat{\Gamma}$ now plays the role of the wave function. Since the $\mathbf{k}$ structure of the Γ^a vertex is very simple, one can classify all solutions of Eq. (31) in terms of the nearest-neighbor s, p, and d waves: $\varphi^s_{\mathbf{k}} = \cos(k_x)+\cos(k_y)$, $\varphi^p_{\mathbf{k}} = \sqrt{2}\sin(k_x)$, $\sqrt{2}\sin(k_y)$, and $\varphi^d_{\mathbf{k}} = \cos(k_x)-\cos(k_y)$. Using the property $\Sigma_{\mathbf{p}}\gamma_{\mathbf{k}-\mathbf{p}}\varphi^{s(p,d)}_{\mathbf{p}} = \frac{1}{4}\varphi^{s(p,d)}_{\mathbf{k}}$, one can see that these solutions are degenerate with energy $\Delta^{s,p,d} = E^{s,p,d} = -J/2$. This is expected if one remembers that while an individual hole breaks four AF bonds, two nearest-neighbor holes save one bond.

A finite hopping constant t has three effects: (i) the hole Green's function becomes renormalized, (ii) Γ^b and Γ^c start to contribute to the interaction, and (iii) the hole self-energy also acquires a small $\mathbf{k}$-dependent contribution. In order to see their roles, let us incorporate these changes into the BS equation (26) one by one.

Consider the case when the hole Green's function is renormalized as described in Sec. III and is $\mathbf{k}$ independent, but the interaction still comes from the Γ^a term only. Since Γ^a is $\mathbf{P}$ and ϵ independent, the BS equation is similar to Eq. (31)

$$\hat{\Gamma}_{\mathbf{k}}(E) = -2J\sum_{\mathbf{p_1}} \gamma_{\mathbf{k}-\mathbf{p_1}}\hat{\Gamma}_{\mathbf{p_1}}(E)\sum_{\epsilon_1} G(E/2+\epsilon_1)G(E/2-\epsilon_1). \tag{32}$$

Since the $\mathbf{k}$ structure of the core is unchanged, all three harmonics remain degenerate. Hence

$$1 = -\frac{J}{2}\sum_{\epsilon_1} G(E/2+\epsilon_1)G(E/2-\epsilon_1). \tag{33}$$

In the lowest-pole approximation G is given by Eq. (29), so the binding energy relative to the bottom of the hole band is

$$\Delta = E - 2\epsilon_0 = -Ja_0^2/2. \tag{34}$$

In the limit $t \ll J$, $\Delta \approx -J(1-16t^2/9J^2)/2$. In the limit $t \gg J$, $a_0 \sim J/t$ so $\Delta \sim -J(J/t)^2$. The binding energy (in units of J) vs t/J is shown in Fig. 12. This energy is always negative because we assume that the hole forms a completely localized excitation. In this case a bound state is always formed as long as the effective interaction remains attractive.

Now we consider the magnon exchange interaction Γ^b, which is given by

$$\Gamma^b_{\mathbf{k},\mathbf{p},\mathbf{P}}(\epsilon,\epsilon_1) = -16t^2\left[\frac{\gamma_{\mathbf{P}/2-\mathbf{p}}\gamma_{\mathbf{P}/2-\mathbf{k}}}{\epsilon+\epsilon_1-2J+i0} + \frac{\gamma_{\mathbf{P}/2+\mathbf{p}}\gamma_{\mathbf{P}/2+\mathbf{k}}}{-\epsilon-\epsilon_1-2J+i0}\right]. \tag{35}$$

Since Γ^b depends on the total momentum of the pair $\mathbf{P}$, the solutions of the BS equation also depends on $\mathbf{P}$. The energy of the bound state at different $\mathbf{P}$ provides a dispersion law for the pair. In general, the lowest-energy bound state is always at zero or some finite momenta corresponding to high-symmetry points in the $\mathbf{k}$ space. In this work we do not consider finite-$\mathbf{P}$ bound states because their physics is unimportant for the purposes of this paper.

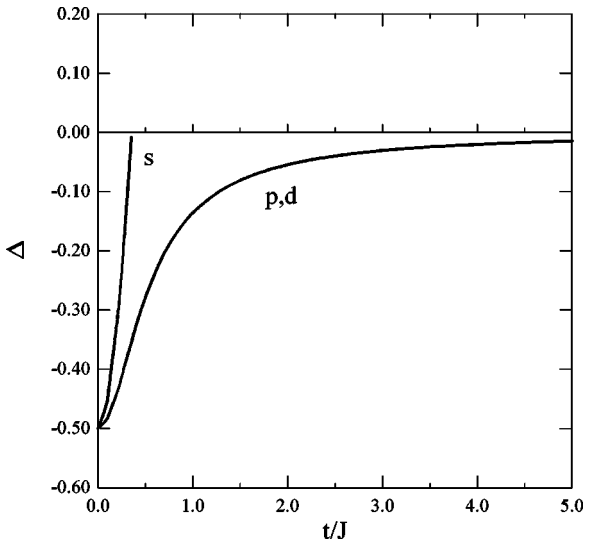

FIG. 12. Binding energies (in units of J) of the s, p, and d bound states. When only the contact interaction Γ^a is taken into account, all three bound states are degenerate [Eq. (34)], and are shown by the lower curve. When the contact and magnon-exchange interactions $\Gamma^a+\Gamma^b$ are considered, the p and d energies are unchanged (lower curve), while the energy of the s state is pushed up [Eq. (40)] (upper curve).

The BS equation (26) at $\mathbf{P}=0$ with interaction $\Gamma^a+\Gamma^b$ reads

$$\hat{\Gamma}_{\mathbf{0},\mathbf{k}}(E,\epsilon) = -2J\sum_{\boldsymbol{\epsilon_1}} G(E/2+\epsilon_1)G(E/2-\epsilon_1) \times\sum_{\mathbf{p}}\left\{\gamma_{\mathbf{k}-\mathbf{p}} + \frac{8t^2}{J}\gamma_{\mathbf{p}}\gamma_{\mathbf{k}}\left[\frac{1}{\epsilon+\epsilon_1-2J+i0} + \frac{1}{-\epsilon-\epsilon_1-2J+i0}\right]\right\}\hat{\Gamma}_{\mathbf{0},\mathbf{p}}(E,\epsilon_1). \tag{36}$$

Evidently, the $\mathbf{k}$ and ϵ dependencies of $\hat{\Gamma}$ can be separated and one can see that the p- and d-wave solutions are not affected by the magnon-exchange interaction because $\Sigma_{\mathbf{p}}\gamma_{\mathbf{p}}\varphi^{p(d)}_{\mathbf{p}} \equiv 0$. This observation can be expressed in a different form: in the zero total momentum p- or d-wave state the amplitudes of the spin-flip exchange from different lobes of the wave function cancel each other.

For the s-wave state, substituting $\hat{\Gamma}_{\mathbf{k}}(\epsilon) = \varphi^s_{\mathbf{k}}\hat{\Gamma}(\epsilon)$ and integrating over $\mathbf{k}$ give

$$\hat{\Gamma}_E(\epsilon) = -\frac{J}{2}\sum_{\epsilon_1} G(E/2+\epsilon_1)G(E/2-\epsilon_1) \times\left\{1 + \frac{8t^2}{J}\left[\frac{1}{\epsilon+\epsilon_1-2J+i0} + \frac{1}{-\epsilon-\epsilon_1-2J+i0}\right]\right\}\hat{\Gamma}_E(\epsilon_1). \tag{37}$$

In the so-called static approximation, when the retardation due to the magnon propagator is neglected, Γ^b is ϵ independent, and Eq. (37) becomes

$$1=-\frac{J}{2}\left\{1-\frac{8t^2}{J}\right\}\sum_{\epsilon_1} G(E/2+\epsilon_1)G(E/2-\epsilon_1)$$
$$\simeq-\frac{J}{2}\frac{a_0^2}{\Delta^s}\left\{1-\frac{8t^2}{J^2}\right\}. \tag{38}$$

As in the previous case, $\Delta^s=E^s-2\epsilon_0$. The problem with retardation can be solved using a method introduced in Ref. 28. One can assume that $\hat{\Gamma}_E(\epsilon)$ has no singularities,[29] and therefore the integral over ϵ_1 in Eq. (37) is defined by the poles of G and the magnon propagator only. In the lowest-pole approximation, by using the obvious parity $\hat{\Gamma}(-\epsilon)=\hat{\Gamma}(\epsilon)$ and by choosing the proper contour of integration, one obtains

$$\hat{\Gamma}_E(\epsilon)=-\frac{J}{2}\frac{a_0^2}{\Delta^s}\left\{1+\frac{8t^2}{J}\left[\frac{1}{\epsilon+\Delta^s/2-2J+i0}+\frac{1}{-\epsilon-\Delta^s/2-2J+i0}\right]\right\}\hat{\Gamma}_E(\Delta^s/2). \tag{39}$$

Multiplying both sides by $G(E/2+\epsilon)G(E/2-\epsilon)$ and integrating over ϵ finally yields

$$1=-\frac{J}{2}\frac{a_0^2}{\Delta^s}\left\{1+\frac{16t^2}{J(\Delta^s-2J)}\right\}. \tag{40}$$

This expression coincides with that given by the Wigner-Brillouin perturbation theory. The resulting binding energies (from $\Gamma^a+\Gamma^b$) vs t/J are shown in Fig. 12.

Thus the s-wave binding energy vanishes at $(t/J)|_c=1/(2\sqrt{2})\simeq 0.35$. Since the spin polarons are assumed to be localized, the disappearance of the bound state is not due to the competition between the delocalizing kinetic energy and an attraction, but rather due to the competition between different types of interaction. One can see that the magnon exchange actually leads to an effective repulsion between the holes. In a naive point of view the holes can be mutually attracted by following each other in a caterpillarlike process, because in this way the disturbance on the AF background is only virtual. However, this scenario does not take into account the fact that after an elementary hopping of a hole pair, the order of the holes is different from the initial one, i.e., they are exchanged.[30] This in turn makes the corresponding energy correction positive, i.e., it leads to repulsion.

It is interesting to note that while the hole-magnon interaction plays a major role in the hole dressing, it has no direct effect on the p and d bound states and is destructive for the s-wave state. The conclusion that the caterpillarlike processes disfavor s waves and leave p and d waves degenerate was reached in Ref. 25 using a different approach.

Let us now add the third part of the hole-hole interaction Γ^c, and see if the combination of the hole-magnon interaction with the two-magnon vertex causes an additional attraction. The diagrams in Fig. 10(c) are equivalent to

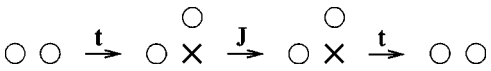

FIG. 13. Real-space image of the process in Fig. 10(c).

$$\Gamma^c_{\mathbf{k},\mathbf{p}}(E,\epsilon,\epsilon_1)=-2J(4t)^2\gamma_{\mathbf{k}-\mathbf{p}}\sum_{\mathbf{q}}\gamma^2_{\mathbf{k}-\mathbf{q}}\times\sum_{\omega}\frac{1}{\omega-2J+i0}\left[\frac{G(\epsilon+E/2-\omega)}{\omega-\epsilon+\epsilon_1-2J+i0}+\frac{G(-\epsilon+E/2-\omega)}{\omega+\epsilon-\epsilon_1-2J+i0}\right]. \tag{41}$$

Integration over the inner momentum $\mathbf{q}$ and frequency ω yields

$$\Gamma^c_{\mathbf{k},\mathbf{p}}(E,\epsilon,\epsilon_1)=-8Jt^2\gamma_{\mathbf{k}-\mathbf{p}}\frac{1}{\epsilon_1-\epsilon}[G(\epsilon+E/2-2J)-G(-\epsilon+E/2-2J)-(\epsilon\rightarrow\epsilon_1)]. \tag{42}$$

One can see that the kinematic structure of this vertex is identical to Γ^a, i.e., this term is effectively a contact nearest-neighbor interaction. This is evident from the real-space picture of the process, which is shown in Fig. 13. Initially the holes are at nearest-neighbor sites. One of them jumps to a neighboring site creating a spin-flip at its site of origin. Then the second hole virtually absorbs and reemits this magnon. Finally the first hole jumps back and the original state is restored. Naturally, such an interaction depends only on $\gamma_{\mathbf{k}-\mathbf{p}}$, and does not depend on $\mathbf{P}$. One can also guess the character of the resulting interaction. Being in the neighborhood of another hole, the spin excitation generated by the hopping of the first hole lowers its energy. Therefore, the interaction between the holes via such a process must also be attractive.

In the lowest-pole approximation Γ^c, Eq. (42) is given by

$$\Gamma^c_{\mathbf{k},\mathbf{p}}(E,\epsilon,\epsilon_1)=-8Jt^2a_0\gamma_{\mathbf{k}-\mathbf{p}}\times\left[\frac{1}{(\epsilon+\Delta/2-2J+i0)(\epsilon_1+\Delta/2-2J+i0)}+(\epsilon,\epsilon_1\rightarrow-\epsilon,-\epsilon_1)\right]. \tag{43}$$

One can consider the static limit of the problem by eliminating the frequency dependence of the propagators in Eq. (43). This gives

$$\Gamma^c_{\mathbf{k},\mathrm{p}}\simeq-4\frac{t^2}{J}a_0\gamma_{\mathbf{k}-\mathbf{p}}. \tag{44}$$

In the $t\gg J$ limit this expression yields $\Gamma^c_{\mathbf{k},\mathbf{p}}\simeq-4t\gamma_{\mathbf{k}-\mathbf{p}}=(2t/J)\Gamma^a_{\mathbf{k},\mathbf{p}}\gg\Gamma^a_{\mathbf{k},\mathbf{p}}$. Thus in this limit the effective interaction constant of the contact interaction is renormalized from J to t. For the p and d waves this gives a bound-state energy $\Delta^{p(d)}\sim-ta_0^2\sim-J(J/t)$, which is a factor of $(t/J)\gg 1$ larger than the result obtained with Γ^a only. This result, while being quite simple, is somewhat unexpected. In a real-space

variational study of the t-J model, a similar effect has been observed in the context of the caterpillarlike movement of holes.[25]

A rigorous account for the retardation yields modified equations for the bound-state energies, leaving the qualitative picture drawn in the static limit essentially unchanged:

$$1=-\frac{J}{2}\frac{a_0^2}{\Delta^{p(d)}}\left\{1+\frac{8t^2a_0}{(\Delta^{p(d)}-2J)^2}\right\},\quad p \text{ and } d \text{ waves},$$

$$1=-\frac{J}{2}\frac{a_0^2}{\Delta^{s}}\left\{1+\frac{8t^2a_0}{(\Delta^{s}-2J)^2}+\frac{16t^2}{J(\Delta^{s}-2J)}\right\},\quad s \text{ wave}. \tag{45}$$

Thus the energies of the p- and d-wave states are always negative. In the s-wave bound state, Γ^c cannot overcome the magnon-exchange repulsion Γ^b. It also has little effect on $(t/J)|_c^s$ because in the small t region where Δ^s goes to zero, Γ^c is roughly four times smaller than Γ^b.

We now consider the effect of the renormalization. As we noted above we have enough reasons to rule out the possibility that the Trugman-like diagrams (Fig. 11) can change the interaction constants significantly. The anticipated smallness of these diagrams in the $t>J$ region is due to the geometrical factor, which is of the order of $1/z^3=1/64$. Most of these corrections are relatively easy to evaluate using the same approximations as above. The results of these calculations show that those terms with the same kinematic structure as in Γ^a, Γ^b, and Γ^c are indeed suppressed by this small factor. They also show that among the corrections there are terms with a more complicated kinematic structure than the original Γ. Since these terms are not suppressed by the small factor, they might enhance the effective interaction. Some of these terms correspond to the contact interaction between the holes in states where both of them have ''tails'' of strings. Evidently, this leads to an interaction of polarons at sites farther than nearest neighbors. For the bound-state wave function this would mean that harmonics higher than the nearest-neighbor one should be considered. Nevertheless, we do not expect these terms to make any qualitative change, and in the following we will omit all corrections from Fig. 11 to avoid complications.

At the same time, diagrams of the non-SCBA type (Fig. 6) are straightforward to include using the real-space language. We have to take into account the lower energy of the magnons in the intermediate state in the diagrams Figs. 10(b) and 10(c). This simply changes $\omega_0=2J$ in the denominators of Eqs. (45) to $\tilde{\omega}_0=J$. Renormalization of the hole energy in the intermediate state in Γ^c produces much weaker effect. This renormalization finally yields

$$\frac{\Delta^{p(d)}}{J}=-\frac{a_0^2}{2}\left\{1+\frac{8t^2a_0}{(\Delta^{p(d)}-J)^2}\right\},$$
$$\frac{\Delta^{s}}{J}=-\frac{a_0^2}{2}\left\{1+\frac{8t^2a_0}{(\Delta^{s}-J)^2}+\frac{16t^2}{J(\Delta^{s}-J)}\right\}. \tag{46}$$

Solutions of these equations are plotted in Fig. 14. One can see that the energies of the p and d bound states are changed significantly from those in Fig. 12. Thus the hierarchy of terms in the effective hole-hole interaction emerged from our study is as follows.

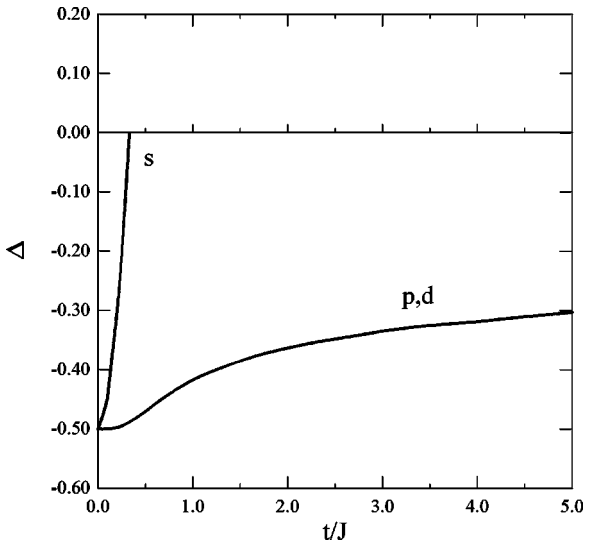

FIG. 14. Binding energies of the s, p, and d bound states when all three interactions shown in Fig. 10 are taken into account and the energy of the magnons in the intermediate state is renormalized.

(i) The contact ''sharing common link'' attraction yields bound states with s, p, and d symmetries with energy $\sim -J/2$ at small t/J.

(ii) The magnon-exchange interaction has no effect on the $\mathbf{P}=0$ p- and d-wave states because of symmetry reasons, and is strongly repulsive for the s-wave state.

(iii) The hole-magnon attraction, which leads to an attraction between a hole and a string of another hole, is the strongest interaction in the present problem in the physical limit $(t>J)$. It leads to deeper p and d bound states with energy $\sim -J(J/t)$.

Now, after all essential interactions are taken into account and carefully analyzed, the last effect which has to be incorporated into the BS equation before we can make a comparison with numerical results is the $\mathbf{k}$-dependent contributions to the hole Green's function. As noted in Sec. III such contributions are small, but lead to a coherent hole band. Therefore the ED data show some dispersion in the hole energy. For instance, at $t/J=5$ the energy difference between the $\mathbf{k}=(0,0)$ and $\mathbf{k}=(\pi/2,\pi/2)$ points (almost exactly half of the bandwidth) is $W/2\simeq 0.078t=0.39J$. Although this difference is small compared to the absolute value of the lowest-pole energy, $\epsilon_0\simeq -2.8t$, or the separation between the energy levels, $\delta\epsilon\sim t$, it is as large as the hole-hole binding energy calculated above, $\Delta\sim -0.3J$. Therefore, one would expect this dispersion to have strong influence on the pairing of holes. One can also foresee that such an influence is likely to be destructive, because now the pairing is not only an interplay between repulsions and attractions, but also the question of how much kinetic energy is lost if the holes are in a bound state.

For our purposes we will need the hole Green's function in the lowest-pole approximation, which now reads

$$G(\epsilon)\approx\frac{a_0}{\epsilon-\tilde{\epsilon}_0-W\epsilon_{\mathbf{k}}/2+i0}, \tag{47}$$

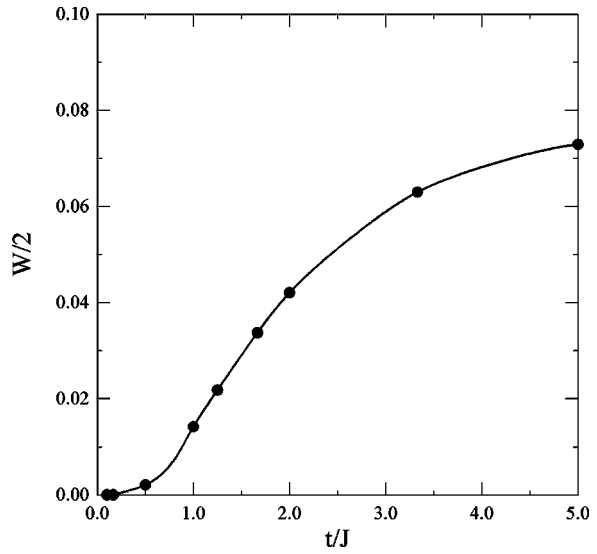

FIG. 15. Half of the hole bandwidth in units of t as the function of t/J.

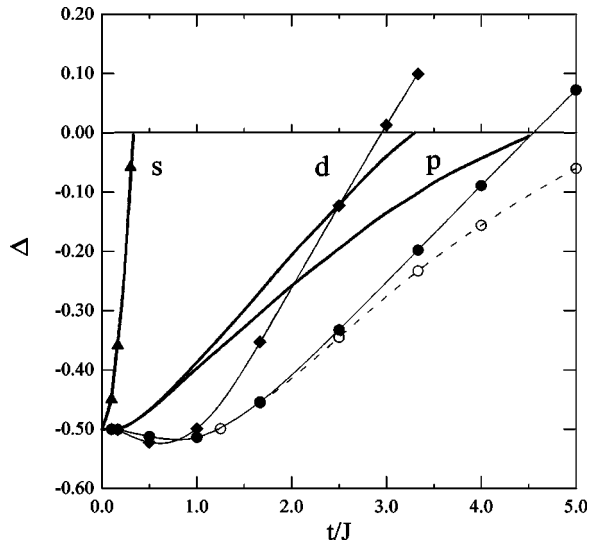

FIG. 16. Binding energies of the s-, p-, and d-wave bound states. Bold lines are the solutions of Eq. (48). Triangles, diamonds, and solid circles are the 32-site ED results for the s, d, and p waves, respectively. Lines connecting these points are guides for the eye. Empty circles are the results of modified Lanczos study on a 50-site cluster from Ref. 24.

where $\tilde{\epsilon}_0=\epsilon_0-W/2$, $\epsilon_{\mathbf{k}}=[1-\cos(k_x)\cos(k_y)]>0$, $W>0$, and we have neglected the $\mathbf{k}$ dependence of a_0. The role of the Trugman's loops larger than an elementary square is negligible, so we consider the dispersion given by the next-nearest-neighbor hopping only. The resulting band is isotropic and has a minimum at the center of the Brillouin zone (BZ). Now in the BS equation (26) it is easier to integrate over ϵ_1 first. Neglecting the effect of the dispersion on the retardation, and after some algebra one obtains

$$\varphi_{\mathbf{k}}=-2Ja_0^2\sum_{\mathbf{p}}\frac{\varphi_{\mathbf{p}}}{\Delta-W\epsilon_{\mathbf{p}}}\left\{\gamma_{\mathbf{k}-\mathbf{p}}\left[1+\frac{8t^2a_0}{(\Delta-J)^2}\right]+\gamma_{\mathbf{k}}\gamma_{\mathbf{p}}\frac{16t^2}{J(\Delta-J)}\right\}. \tag{48}$$

where $\varphi_{\mathbf{k}}$ is a nearest-neighbor s, p, or d wave. As before the magnon-exchange interaction (the second term in the curly bracket) is orthogonal to the p- and d-wave states. Equation (48) is an almost evident generalization of Eqs. (46) to the case of finite hole dispersion. The only new parameter introduced is the hole bandwidth W. Our numerical ED data for $W/2t$ as a function of t/J calculated on a 32-site lattice are given in Fig. 15. We do not calculate this quantity analytically. Instead we treat it as a parameter and use the numerical values in Fig. 15.

Two statements can be made about the solutions of Eq. (48). Now all three symmetries have thresholds $(t/J)|_c^{s,p,d}$ above which negative energy solution of the corresponding symmetry cease to exist. Also, the p and d waves are split with the p wave state having lower energy.

The first statement is evident if one considers the threshold condition $(\Delta=0)$ for the p- or d-wave state in Eq. (48), assuming $t\gg J$ so that $a_0\simeq J/t$:

$$1\simeq-\frac{J}{2}\frac{J^2}{t^2}\sum_{\mathbf{p}}\frac{\varphi_{\mathbf{p}}^{p,d}}{-W\epsilon_{\mathbf{p}}}\left\{1+\frac{8t^2}{J^2}\frac{J}{t}\right\}\simeq\frac{4J}{W}\frac{J}{t}\sum_{\mathbf{p}}\frac{\varphi_{\mathbf{p}}^{p,d}}{[1-\cos(k_x)\cos(k_y)]}. \tag{49}$$

The sum over $\mathbf{p}$ gives a number of the order of unity. Thus, there is a value of $W[(W/t)_c\simeq 4J^2/t^2\ll 1]$ at which the equality condition is satisfied. If W grows with t, as it in fact does, then above this point Eq. (48) has no solution. Using the dependence of W on t/J (Fig. 15), the critical values of $t/J|_c^{p,d}$ can be extracted from the same condition Eq. (49).

The second statement is a consequence of the isotropic form of the dispersion law. The sum over $\mathbf{p}$ in Eq. (49) can be rewritten as:

$$A^{p,d}=\sum_{\mathbf{p}}\frac{\varphi_{\mathbf{p}}^{p,d}}{\epsilon_{\mathbf{p}}}=\sum_{\mathbf{p}}\varphi_{\mathbf{p}}^{p,d}\{1+\cos(k_x)\cos(k_y)+[\cos(k_x)\cos(k_y)]^2+\cdots\}=1+C_1+C_2+\cdots. \tag{50}$$

In the case of d wave the series is alternating with $C_1=-\frac{1}{2}$ and $C_2=\frac{3}{8}$. In the case of p wave $C_n\equiv 0$ for odd n, and $C_n>0$ for even n. Numerical integration gives $A^p=1.27$ and $A^d=0.73$, and therefore the d-wave solution disappears at a lower value of t/J.

Numerical solutions of Eq. (48) for all three symmetries together with results of our 32-site ED calculations are shown in Fig. 16. For the purpose of comparison we also show the results obtained by a modified Lanczos method on a 50-site cluster in Ref. 24. One can see a very good *quantitative* agreement between our analytical and numerical results for the s-wave state. For the d and p states, they have the same qualitative behaviors. It is clear that our Eq. (48), while involving different kinds of approximations, captures all essential effects of the pairing problem in the t-J_z model in a very good quantitative level. It also describes the problem in a very easy and transparent way. That is, all essential tendencies in the hole binding are described by this formula: (i) the s wave is pushed up to the continuum by the magnon-exchange process, (ii) the p and d waves are much more

stable, and (iii) the Trugman's dispersion splits these two levels and pushes them to the continuum at some larger critical values of t/J.

The analytical results underestimate the pairing strength, especially in the region $t/J\sim 1$. We believe that this is due to the contribution from the higher poles which are neglected in our study. In this region a significant portion of the spectral weight is transferred to these poles, while the separation between them is still of the order of $2J$. Since our lowest-pole approximation uses the ratio $\Delta/\delta\epsilon(\simeq 1/4$ in this region) as the small parameter, one would expect the energy correction from the higher poles to be of the same order. In the region where the binding energy is close to zero we expect this approximation to be more accurate. However, for the p and d waves this is also the region of $t/J>2$ where the omitted higher-order diagrams with more complicated kinematic structure contribute to the interaction. We refer the smaller splitting of the p- and d-wave states found in our analytical results compared to those in our ED data to the effect of these corrections. The same higher-order interactions cause a tiny splitting of the states at $t/J<1$, which is shown in Fig. 16. We remark that a t/J dependence of the binding energies very similar to our ED results has been found recently by series-expansion calculations.[31] Thus we believe that the agreement between the results can be improved by an accurate consideration of the contribution of higher poles and higher-order diagrams of various types. However, this is beyond of the scope of our paper.

It is natural and instructive to consider the case where small transverse spin fluctuations $J_\perp=\alpha J$ (with $\alpha\ll 1$) are included in the Hamiltonian. This helps one to see the effects of these fluctuations on the pairing problem, and to infer the tendencies in the isotropic t-J model. As noted in Ref. 18 only two changes are necessary to account for these fluctuations up to first order in α. First, the holes acquire a dispersion law given by

$$\delta\epsilon_{\mathbf{k}}=\alpha A\gamma_{\mathbf{k}}^2, \tag{51}$$

where A is of the order of t^2/J in the $t\ll J$ limit and of the order of J in the $t\gg J$ limit.[18] Such a band is strongly anisotropic, i.e., degenerate minima form a line along the magnetic BZ boundary. In the full t-J model ($\alpha=1$) this dispersion dominates over the Trugman's terms at all t/J. Second, the hole-magnon interaction becomes

$$\Gamma_{\mathbf{k},\mathbf{q}}^{(1)}=4t[\,\gamma_{\mathbf{k}-\mathbf{q}}-\tfrac{1}{2}\alpha\gamma_{\mathbf{k}}\gamma_{\mathbf{q}}+O(\alpha^2)]. \tag{52}$$

Corrections to the magnon energy are of higher order in α: $\omega_0=2J+O(\alpha^2)$. As we shall see, both changes lead to the splitting of the p- and d-wave levels, and both favor the d wave as the ground state of the system.

Consider Eq. (48) with the dispersion from Eq. (51) and the hole-magnon exchange term coming from Eq. (52). For the purpose of illustration it is sufficient to consider the interactions in the static limit:

$$\varphi_{\mathbf{k}}=-2Ja_0^2\sum_{\mathbf{p}}\frac{\varphi_{\mathbf{p}}}{\Delta-2\alpha A\gamma_{\mathbf{p}}^2}\left\{\gamma_{\mathbf{k}-\mathbf{p}}\left[1+\frac{8t^2a_0}{J^2}\right]-\frac{16t^2}{J^2}\left[\gamma_{\mathbf{k}}\gamma_{\mathbf{p}}-\frac{\alpha}{2}\gamma_{\mathbf{k}+\mathbf{p}}(\gamma_{\mathbf{k}}^2+\gamma_{\mathbf{p}}^2)\right]\right\}. \tag{53}$$

Corrections to the bound-state energies of the p and d waves up to first order in α are

$$\begin{aligned}\Delta^d&=\Delta_0^d+2\alpha\left(A-\frac{2t^2}{J}a_0^2\right)\sum_{\mathbf{p}}(\varphi_{\mathbf{p}}^d)^2\gamma_{\mathbf{p}}^2\\&=\Delta_0^d+\frac{\alpha}{8}\left(A-\frac{2t^2}{J}a_0^2\right),\\\Delta^p&=\Delta_0^p+2\alpha\left(A+\frac{2t^2}{J}a_0^2\right)\sum_{\mathbf{p}}(\varphi_{\mathbf{p}}^p)^2\gamma_{\mathbf{p}}^2\\&=\Delta_0^p+\frac{3\alpha}{8}\left(A+\frac{2t^2}{J}a_0^2\right),\end{aligned} \tag{54}$$

where the first term in the bracket comes from the dispersion and the second is from the magnon-exchange interaction. The kinetic energy pushes up the energy of both states, but for the p wave this shift is three times larger. An important observation is that the magnon-exchange interaction is now attractive for the d-wave state and repulsive for the p-wave state.

To show how subtle the selection between the p- and d-wave ground states is, let us consider a more ''realistic'' dispersion law:

$$\delta\epsilon_{\mathbf{k}}=\frac{\alpha}{4}A[\cos(k_x)^2+\cos(k_y)^2]. \tag{55}$$

This is more realistic in the sense that it has minima at $\pm(\pm\pi/2,\pi/2)$ points which are isotropic and it agrees with the experimentally measured profile in the cuprates better than the one in Eq. (51). It is now known that this difference between the t-J model dispersion law [Eq. (51)] and the one observed in reality [Eq. (55)] is due to additional intrasublattice hoppings (t',t'', etc.) in the real systems.[5] With the dispersion law in Eq. (55), corrections to the binding energies are given by

$$\Delta^d=\Delta_0^d+\frac{\alpha}{8}\left(5A-\frac{2t^2}{J}a_0^2\right),\quad \Delta^p=\Delta_0^p+\frac{\alpha}{8}\left(3A+\frac{2t^2}{J}a_0^2\right). \tag{56}$$

Now the kinetic energy pushes up the d-wave energy 5/3 times more than that of the p-wave energy, and $\Delta^p-\Delta^d=(\alpha/4)[2t^2a_0^2/J-A]$ is not necessarily positive. Therefore, the p wave can again become a ground state.

Summarizing our observations in the small-α limit, we conclude that the transverse fluctuations create an additional attractive interaction in the d-symmetry state and that an anisotropic kinetic-energy profile also favors the d wave. Thus we suggest that the d wave is most likely to be the ground state of the system in the t-J model ($\alpha=1$). This conclusion is in agreement with many analytical and numerical studies. Nevertheless, a recent 32-site ED study showed that at $t/J>3.3$ the ground state of the two-hole t-J model is a p-wave state with total momentum $\mathbf{P}=(\pi,\pi)$.[32] [In our case momenta $\mathbf{P}=(0,0)$ and $\mathbf{P}=(\pi,\pi)$ are equivalent because of the existence of long-range order.] Furthermore, such a behavior is also suggested by recent series-expansion calculations.[31] Due to the apparently strong finite-size effects on the ED results, it is difficult to conclude whether this behavior will

survive in the thermodynamic limit. Nevertheless, these data show that even in the pure t-J model, the final word on the problem of the symmetry of the bound state is still to come.

Besides effects arising from the t-J model, there are also concerns about the robustness of the bound states in the real system. The characteristic bound-state energy found in the t-J model is of the order of $-0.1J$ in the physical region of t/J. This energy is far below the accuracy of the model itself. This means that in order to describe the real materials, the low-energy model must include at least additional hopping terms (t',t'', etc.). It is worth noting again that because of these terms the realistic dispersion is isotropic, which, as we have just shown, can favor the p wave. More important conjecture can be made using the results of Ref. 28 and ED data.[33] Since the isotropic dispersion involves a higher kinetic energy, the overall pairing tendency is weakened by these additional hopping terms. It can push all the bound states up to the continuum, thus destroying the foundation of the preformed pair and phase separation scenarios well before the physical region of parameters is reached.

VI. CONCLUSIONS

In this paper we attempt to address the issue of how generic d-wave pairing in t-J-like models is, and to clarify the problem of how this symmetry is selected among others. We have thoroughly examined the t-J_z model by means of analytical diagrammatic study supplemented by our 32-site ED results. This formalism is tested in the one-hole problem, and perfect agreement with ED results is found. The ground state of two holes in the physical region $t/J>1$ is found to be a p-wave bound state. From a careful analysis of the interactions involved in the pairing problem we established that the pairing in the s-wave channel is highly unfavorable because of the repulsive character of the magnon-exchange interaction in this state. While this reason is rather generic, the problem of selecting between the p and d waves is much more subtle. In our analytical study these states remain degenerate until the hole dispersion is included. In the t-J_z model such a dispersion comes from higher-order hopping processes, and is, in fact, very small. However, it has important consequences. It is responsible not only for the significant splitting between the p- and d-wave states, but also for the destruction of hole pairing at some critical $(t/J)|_c^{p,d}$. The isotropic form of the dispersion favors the p wave as the ground state of the system.

We have also considered the role of transverse fluctuations in the perturbative limit $\alpha \ll 1$. These lead to an anisotropic hole dispersion and an additional hole-hole interaction. We have shown that both features favor the d wave as the lowest energy state. However, in this case the selection between p and d waves strongly relies on the anisotropic form of the hole dispersion, and such a dispersion does not agree with the experimentally measured dispersion in real systems. Moreover, since the characteristic energy of the bound states found in the t-J models is small, we are skeptical that these states can survive when additional kinetic-energy terms are included in the model. Our skepticism is supported by earlier studies[28] and recent numerical data.[34,33]

Such conclusions for the pairing problem in t-J-like models drawn from our study create a framework in which it might be necessary to look for d-wave superconductivity unrelated to the Bose condensation of preformed d-wave pairs. Furthermore, to make the phase-separation scenario possible, one might need to invoke arguments other than an *a priori* existing collapsing tendency in the spin-hole system.

ACKNOWLEDGMENTS

We are indebted to Professor R. J. Gooding for suggesting this work, and for valuable discussions and comments. We also thank F. Marsiglio for illuminative discussion, A. Castro Neto, M. Zhitomirsky, and O. Starykh for comments, and P. Wrobel for correspondence. The work of A.L.C. was supported in part by the NSERC of Canada and the University of California and Los Alamos National Laboratory under the auspices of the U.S. Department of Energy. The work of P.W.L. was supported by the Hong Kong RGC grant HKUST6144/97P. Numerical diagonalizations of the 32-site systems were performed on the Intel Paragon at HKUST.

*On leave from the Institute of Semiconductor Physics, Novosibirsk, 630090, Russia.

[1] P.W. Anderson, Science **235**, 1196 (1987).
[2] F.C. Zhang and T.M. Rice, Phys. Rev. B **37**, 3759 (1988).
[3] J.H. Jefferson, H. Eskes, and L.F. Feiner, Phys. Rev. B **45**, 7959 (1992); M.E. Simon and A.A. Aligia, *ibid.* **48**, 7471 (1993); V.I. Belinicher and A.L. Chernyshev, *ibid.* **49**, 9746 (1994); V.I. Belinicher, A.L. Chernyshev, and L.V. Popovich, *ibid.* **50**, 13 768 (1994); V.I. Belinicher, A.L. Chernyshev, and V.A. Shubin, *ibid.* **53**, 335 (1996).
[4] B.O. Wells, Z.-X. Shen, A. Matsuura, D. M. King, M. A. Kastner, M. Greven, and R. J. Birgeneau, Phys. Rev. Lett. **74**, 964 (1995).
[5] A. Nazarenko, K.J.E. Vos, S. Haas, E. Dagotto, and R.J. Gooding, Phys. Rev. B **51**, R8676 (1995); P.W. Leung, B.O. Wells, and R.J. Gooding, *ibid.* **56**, 6320 (1997).
[6] V.I. Belinicher, A.L. Chernyshev, and V.A. Shubin, Phys. Rev. B **54**, 14 914 (1996).
[7] For a recent review, see E. Dagotto, Rev. Mod. Phys. **66**, 763 (1994).
[8] E. Dagotto and J. Riera, Phys. Rev. Lett. **70**, 682 (1993).
[9] Y. Ohta, T. Shimozato, R. Eder, and S. Maekawa, Phys. Rev. Lett. **73**, 324 (1994).
[10] L.N. Bulaevskii, E.L. Nagaev, and D.I. Khomskii, Zh. Éksp. Teor. Fiz. **54**, 1562 (1968) [Sov. Phys. JETP **27**, 836 (1968)].
[11] W.F. Brinkman and T.M. Rice, Phys. Rev. B **2**, 1324 (1970).
[12] R. Strack and D. Vollhardt, Phys. Rev. B **46**, 13 852 (1992); W. Metzner, P. Schmit, and D. Vollhardt, *ibid.* **45**, 2237 (1992).
[13] C.L. Kane, P.A. Lee, and N. Read, Phys. Rev. B **39**, 6880 (1988).
[14] S. Schmitt-Rink, C.M. Varma, and A.E. Ruckenstein, Phys. Rev. Lett. **60**, 2793 (1988); F. Marsiglio, A.E. Ruckenstein, S. Schmitt-Rink, and C.M. Varma, Phys. Rev. B **43**, 10 882 (1991).
[15] G. Martínez and P. Horsch, Phys. Rev. B **44**, 317 (1991); Z. Liu and E. Manousakis, *ibid.* **45**, 2425 (1992); **51**, 3156 (1995).
[16] J. Bala, A.M. Oleś, and J. Zaanen, Phys. Rev. B **52**, 4597 (1995).
[17] G. Reiter, Phys. Rev. B **49**, 1536 (1994).
[18] O.A. Starykh and G.F. Reiter, Phys. Rev. B **53**, 2517 (1996).
[19] S. Trugman, Phys. Rev. B **37**, 1597 (1988).
[20] B. Shraiman and E. Siggia, Phys. Rev. Lett. **60**, 740 (1988).

[21] R. Eder, Phys. Rev. B **45**, 319 (1992); P. Wrobel and R. Eder, *ibid.* **49**, 1233 (1994).
[22] A. Chernyshev, A. Dotsenko, and O. Sushkov, Phys. Rev. B **49**, 6197 (1994).
[23] T. Barnes, E. Dagotto, A. Moreo, and E.S. Swanson, Phys. Rev. B **40**, 10 977 (1989).
[24] J.A. Riera and E.P. Dagotto, Phys. Rev. B **47**, 15 346 (1993).
[25] P. Wrobel and R. Eder, Phys. Rev. B **58**, 15 160 (1998).
[26] P.W. Leung and R.J. Gooding, Phys. Rev. B **52**, R15 711 (1995).
[27] A.L. Chernyshev, P.W. Leung, and R.J. Gooding, Phys. Rev. B **58**, 13 594 (1998).
[28] V.I. Belinicher, A.L. Chernyshev, and V.A. Shubin, Phys. Rev. B **56**, 3381 (1997).
[29] The true assumption is weaker. One can require $\hat{\Gamma}(\epsilon)$ to be the sum of a constant term and singular terms, the latter having poles far from the poles of the hole Green's functions in the integral. Approximating $\hat{\Gamma}(\epsilon)$ by the constant term is valid provided that $\Delta/2J \ll 1$.
[30] The authors are grateful to Frank Marsiglio for raising this question.
[31] C.J. Hamer, Z. Weiheng, and J. Oitmaa, Phys. Rev. B **58**, 15 508 (1998).
[32] P.W. Leung (unpublished).
[33] P.W. Leung (unpublished).
[34] T. Tohyama, C. Gazza, C. T. Shih, Y. C. Chen, T. K. Lee, S. Maekawa, and E. Dagotto, Phys. Rev. B **59**, R11649 (1999).